DMD Fast Forward. Published on February 2, 2006 as doi:10.1124/dmd.105.007559

Title Page

Title:

Effect of P-glycoprotein on intestinal absorption and brain penetration of anti-allergic agent bepotastine besilate

Authors:

Rikiya Ohashi, Yukari Kamikozawa, Mika Sugiura, Hajime Fukuda, Hikaru Yabuuchi, and Ikumi Tamai

Institution:

Exploratory DMPK, Exploratory Toxicology and DMPK Research Laboratories, Tanabe Seiyaku Co., Ltd., Saitama, Japan (R.O., Y.K., M.S., H.F.); GenoMembrane, Inc., Yokohama, Japan (H.Y.), and Department of Molecular Biopharmaceutics, Faculty of Pharmaceutical Sciences, Tokyo University of Science, Noda, Japan (I.T.)

Running title page

Running title:

Role of P-gp in pharmacokinetics of bepotastine

Address correspondence to:

Rikiya Ohashi

Exploratory DMPK, Exploratory Toxicology and DMPK Research Laboratories, Tanabe Seiyaku Co., Ltd., 2-2-50, Kawagishi, Toda, Saitama 335-8505, Japan.

Tel: +81-48-433-8111, Fax: +81-48-433-8170

E-mail: r-ohashi@tanabe. co.jp

The number of

Text page: 32

Tables: 3

Figures: 5

References: 38

The number of words in Abstract: 249

Introduction: 518

Discussion: 1541

Abbreviations:

P-gp, P-glycoprotein: BBB, blood-brain barrier: CFR, corrected flux ratio: CMC, carboxymethyl cellulose: LC-MS, liquid chromatography mass spectrometry: Papp, apparent permeability coefficient: ESI, electrospray ionization: WT, wild-type: P-gp KO, mdr1a/1b(-/-): Kp,f, brain-to-plasma free concentration ratio: *ka*, apparent first-order absorption rate constant.

ABSTRACT

The anti-allergic agent bepotastine besilate is a non-sedating, second-generation H1-antagonist with high oral absorption and negligible distribution into brain. To clarify the role of P-gp in the pharmacokinetics of bepotastine, the intestinal absorption and brain penetration studies were performed. [^{14}C]Bepotastine transport in P-gp overexpressed LLC-PK1 cells indicated that bepotastine was a substrate of P-gp. The affinity of bepotastine to P-gp estimated by ATPase activity assay was low with Km value of 1.25 mM. Following intravenous administration, the brain-to-plasma free concentration ratio in mdr1-knockout mice was three times higher than that in wild-type mice. The *in situ* intestinal absorption studies of [^{14}C]bepotastine in rats demonstrated a clear regional difference, showing highest permeability at upper part of small intestine with a decreasing permeability in descending part of small intestine. The apparent absorption rate constant (*ka*) of [^{14}C]bepotastine in the small intestine was greatly increased by cyclosporin A and verapamil, especially in the distal portion, and the site-specific absorption of [^{14}C]bepotastine disappeared. The concentration dependence of *ka* of [^{14}C]bepotastine was observed with a higher *ka* at higher concentration (20 mM) compared with that at lower concentration (1 μM). In conclusion, bepotastine is a substrate for P-gp and P-gp clearly limited the brain distribution of bepotastine, while the effect of P-gp on intestinal absorption of bepotastine was minimal presumably due to high membrane permeability at the upper region of small intestine where P-gp is less expressed. Such intestinal absorption property of bepotastine is distinctly different from the low membrane permeable P-gp substrate fexofenadine.

Introduction

First-generation H1-receptor antagonists have been used for the treatment of allergic disorders. However, they have a problem by inducing sedation, because they penetrated well to the brain (Nicholson 1983, Tagawa et al., 2001). Bepotastine besilate, ((+)-(S)-4-{4-[(4-chlorophenyl)(2-pyridyl)methoxy]piperidino}butyric acid monobenzenesulfonate, betotastine besilate, TAU-284, Talion®) was developed as a second-generation H1-antagonist. Bepotastine showed a high selectivity and potent antagonistic action to H1-receptor, and exerted excellent anti-allergic action (Honda et al., 1997; Kato et al., 1997; Sakai et al., 1997; Yato et al., 1997). Non-clinical and clinical studies suggested that bepotastine does not exhibit the sedation at the clinical therapeutic dose because of limited distribution into brain (Ohashi et al., 1997; Kadosaka et al., 1997). Bepotastine is metabolically stable in dogs and humans and is excreted into urine in an unchanged form more than 70% of dose after oral administration. Intestinal absorption of bepotastine was > 85%, > 70%, and > 80% in rats, dogs and humans, respectively, showing high absorption. The variation of drug concentration in plasma after oral administration to healthy volunteers was small and plasma concentration was not significantly affected by food. The tissue distribution studies of [^{14}C]bepotastine after oral administration to rats showed that [^{14}C]bepotastine distributed widely in the whole body, while its brain distribution was lower than those of ketotifen, terfenadine, and its carboxylic metabolite (fexofenadine) (Kato et al., 1997).

The *MDR1* gene (multidrug resistance; ABCB1) product P-glycoprotein (P-gp) plays an important role in pharmacokinetics of drugs. P-gp is well known as one of important factor to limit membrane permeability in several tissues and/or the elimination pathways into urine and bile. P-gp is highly expressed in the endothelial cells of brain capillaries and restricts the brain penetration of drugs (Tsuji et al., 1992; Schinkel et al., 1994). Although intestinal P-gp is likely a limiting factor of intestinal absorption of drugs, it is also true that substrates of P-gp exhibit good bioavailability (Varma et al., 2005). So, the effect of P-gp on intestinal drug absorption is controversial as compared with those on brain distribution of drugs (Lin and Yamazaki, 2003).

Non-sedative second-generation H1-antagonists such as fexofenadine, ebastine and its metabolite (carebastine) are substrates of P-gp, and limited brain distribution of these drugs has been explained by the efflux transport by P-gp at the blood-brain barrier (BBB) (Cvetkovic et al., 1999; Tamai et al., 2000; Tahara et al., 2005). The oral absorption of fexofenadine and ebastine in rats was estimated using radiolabeled compounds to be about 30% and 50% of dose, respectively (Common Technical Document for the registration of Pharmaceuticals for Human Use; Fujii et al., 1994). Accordingly, the impact of P-gp on the drug absorption may not be high compared with that on the BBB and this point has been already discussed previously (Lin and Yamazaki, 2003).

In the present study, we examined the comparative effects of P-gp on the intestinal absorption and brain distribution of bepotastine, which was clarified to be a substrate of P-gp in the present study, by various *in vitro* and *in vivo* methods and by comparing the P-gp effect on bepotastine and fexofenadine. The structures of bepotastine and fexofenadine are shown in Fig.1.

Materials and Methods

Chemicals. [^{14}C]Bepotastine besilate ([^{14}C] (+)-(S)-4-{4-[(4-chlorophenyl)(2-pyridyl)methoxy] piperidino}butyric acid monobenzenesulfonate) (1.15 GBq/mmol) was synthesized by Amersham Biosciences UK, Ltd. (Little Chalfont, Buckinghamshire, UK). Unlabelled bepotastine besilate was supplied by Ube Industries, Ltd. (Yamaguchi, Japan). [^{3}H]Digoxin and [^{14}C]D-mannitol (2.07 GBq/mmol) were from PerkinElmer (Boston, MA) and Moravek Biochemicals Inc. (Brea, CA), respectively. Fexofenadine hydrochloride, verapamil hydrochloride, and diphenhydramine hydrochloride were purchased from Sigma Chemical Co. (St. Louis, MO, USA). Quinidine sulfate dihydrate and cyclosporin A were purchased from Wako Pure Chemical Industries (Osaka, Japan). P-gp expressing membranes (High Five ,BTI-TN5B1-4) were purchased from GENTEST (Woburn, MA) and ABC Transporter ATPase Assay Reagents Kit was purchased from Nacalai Tesque (Kyoto, Japan). All other chemicals and regents were commercial product of reagent grade.

LLC-PK1 and LLC-GA5-COL150. LLC-PK1 cells were obtained from Japan Health Science Research Resources Bank (Osaka, Japan). LLC-GA5-COL150 cells were purchased from Riken Gene Bank (Tsukuba, Japan). LLC-GA5-COL150 cells were established by transfection of human MDR1 cDNA into LLC-PK1 cells (Tanigawara et al., 1992; Ueda et al., 1992) and were maintained by serial passage in plastic culture dishes. LLC-PK1 cells were incubated in complete medium consisting of Medium 199 (Nissui Pharmaceutical, Tokyo, Japan) with 3% fetal bovine serum (Invitrogen). For LLC-GA5-COL150 cells, 150 ng/mL of colchicine was added to the complete medium consisting of Medium 199 with 10% fetal bovine serum. LLC-PK1 and LLC-GA5-COL150 cells were seeded in plastic dishes containing complete medium. Monolayer cultures were grown at 37°C in a 5% CO_2, 95% air atmosphere.

Transcellular Transport Study in LLC-GA5-COL150 and LLC-PK1 Cells. LLC-PK1 and LLC-GA5-COL150 cells were seeded on microporous polycarbonate membrane Transwells (3-μm pore size, 6.5-mm diameter; Costar, Cambridge, MA) at a cell density of 1.0 x 10^5 and 6.5 x 10^5 cells/cm^2, respectively. Cells were cultured on the microporous membrane with 1.0 and 0.2 mL of complete medium without colchicine in the donor and receiver compartments 24 hours before experiments, respectively. Cells were supplemented with fresh medium on the every two days and used for the transport studies on the sixth day after seeding. About 1 hour before the initiation of the transport experiments, the medium in both the donor and receiver compartments was replaced with transport medium. The transport experiments were initiated by replacing the medium with medium containing or not containing a test compound. After 2 hours, aliquots of medium were taken from the receiver compartment. The drug concentrations were measured in a liquid scintillation counter ([^{14}C]bepotastine, [^{3}H]digoxin, and [^{14}C]D-mannitol) or LC-MS system (fexofenadine). To examine the inhibitory effect of P-gp inhibitors such as cyclosporin A and verapamil on the P-gp-mediated transport in LLC-GA5-COL150 cells, they were added to the medium on the same sides with bepotastine in the cell monolayers at the same time with bepotastine. The paracellular leakage was monitored in terms of the permeability of [^{14}C]mannitol. The apparent permeability coefficient (Papp; cm/sec) was calculated as described previously (Artursson 1990). The flux ratio was calculated by following equations;

$$\text{Flux ratio} = \text{Papp (B-to-A)} / \text{Papp (A-to-B)}$$

where Papp (B-to-A) and Papp (A-to-B) represent the apparent permeability coefficients in the basal-to-apical direction and the apical-to-basal direction, respectively. In LLC-PK1/LLC-GA5-COL150 cells, the corrected flux ratio (CFR) was evaluated by following equations (Adachi et al. 2001);

$$\text{CFR} = (\text{flux ratio in LLC-GA5-COL150}) / (\text{flux ratio in LLC-PK1})$$

Drug-Stimulated P-gp ATPase Activity Assay. The drug-stimulated P-gp ATPase activity was estimated using ABC Transporter ATPase Assay Reagents Kit (Nacalai). Human P-gp membranes (20 μg) were pre-incubated at 37 ℃ for 5 min in 40 μL reaction buffer and each test compound in the presence or absence of 50 μM sodium orthovanadate in 96-well plate. The reaction was initiated by the addition of 20 μL of 12 mM MgATP solution and was terminated 30 min later by the addition of 30 μL of stop solution (10w/v% LDS). 200 μL of detection reagent (8% ascorbic acid, 0.8% ammonium molybdate, 3 mM zinc acetate) were added and incubated at 37 ℃ for 20 min. The inorganic phosphate complex was detected by its absorbance at 750 nm and was quantitated by comparing the absorbance to a phosphate standard. The vanadate sensitive ATP hydrolysis was determined by subtracting the value obtained with the vanadate co-incubated membrane fraction from vanadate-free membrane fraction. To estimate the kinetic parameters, ATP hydrolysis rate (v) was fitted to the following equations by means of nonlinear least-squares regression analysis using WinNonlin (Scientific Consulting Inc., Cray, NC).

$$v = Vmax \times s / (Km + s)$$

where v and s are ATP hydrolysis rate and concentration of P-gp substrate, respectively. The Km and Vmax are the half-saturation concentration (Michaelis constant) and maximum ATP hydrolysis rate, respectively.

Whole-Body Autoradiography of [^{14}C]Bepotastine in P-gp KO and WT Mice. P-gp KO-, and wild-type mice were sacrificed at 60 min after intravenous administration of [^{14}C]bepotastine (0.8 mg/45 μCi/kg), the hair was rapidly clipped, and the nasal cavity and anus were filled with 5% carboxymethyl cellulose sodium (CMC-Na). The carcass was frozen in a dry ice-acetone mixture. The frozen carcass was embedded in 5% CMC-Na on a microtome stage, frozen again in a dry ice-acetone mixture, and held in a Cryomacrocut (Leica, Tokyo, Japan). Then, 40 μm thick sections were cut, collected onto an adhesive tape (No. 810, Sumitomo 3M), and lyophilized. The sections were covered with protective

membranes (4 μm, Dia Foil, Mitsubishi Polyester Film) and placed in contact with imaging plates (TYPE BAS-III, Fuji Photo Film). The plates were exposed at room temperature for 24 hours in lead shield boxes. After exposure, image of radioactivity on the imaging plates was analyzed using BAS2000 (Fiji Photo Film, Tokyo, Japan).

Plasma-Brain Disposition of [^{14}C]Bepotastine in P-gp KO and WT Mice. FVB/NJ (WT) and *mdr1a/1b* gene-deficient (P-gp KO) mice were purchased from Jackson Laboratories (Bar Harbor, ME) and Taconic Farms, Inc. (Germantown, NY), respectively. [^{14}C]Bepotastine (0.8 mg/45 μCi/kg) dissolved in saline solution in a total volume of 100 μL was administered by i.v. bolus injection. At 6 and 60 min after dosing, the mice were sacrificed under ether anesthesia. Mice were immediately dissected and blood and brain samples were collected. Plasma samples were obtained by centrifuging the blood samples at 15,500 x g for 3 min. Brain was rinsed with saline and was separated into cerebrum and cerebellum. The separated brain was blotted dry and weighed. Plasma unbound fraction was determined by ultrafiltration of plasma by using a Microcon YM-10 (Millipore Co., Bedford, MA). The samples associated with brain and plasma was solubilized in Soluene-350 at 60°C for 3 hours and the associated radioactivity was measured by liquid scintillation counting.

***In Situ* Closed Loop Method.** Male Sprague-Dawley rats weighing 220 to 300 g (Charles River Japan, Kanagawa, Japan) were anesthetized with diethylether. An abdominal incision was carefully made to expose the intestinal tissue. The closed loop was made at stomach, small intestine (proximal, mean and distal region) and colon, which was 8-cm length. The intestinal contents were expelled from the respective segments and the segments were flushed with prewarmed (37°C) isotonic phosphate-buffered saline. Following this procedure, 0.25 mL of [^{14}C]bepotastine besilate (1 μM , 2 mM and 20 mM) and fexofenadine hydrochloride (370 μM) in 0.5% CMC in the absence or presence of 2% dimethylsulfoxide

were introduced into a divided segments and both ends of the segment were ligated. The intestinal segment was kept in the body for 30 min during the absorption experiments with a heating lamp to maintain the temperature of the preparation at 37°C. After 30 min, the gastrointestinal loop was collected and was rinsed with saline. After addition of saline to total volume of 10 mL, the loops were homogenized using a Polytron homogenizer. Furthermore, these homogenate were diluted with methylalcohol to the total volume of 40 mL. The residual amount of [^{14}C]bepotastine besilate and fexofenadine hydrochloride in the intestinal lumen was determined by liquid scintillation counting or LC-MS measurement to estimate the absorption rate (% of dose) and the apparent first-order absorption rate constant, *ka* (hr^{-1}). The *ka* value was calculated by following equation;

$$ka = -\ln (A / B) / t$$

where *A* and *B* are amount of substances after and before the initiation of absorption experiment in the intestine, and *t* is the absorption time after injection of substances.

LC-MS quantification of fexofenadine. The LC-MS system consisted of an LC pump, autosampler, thermostated column compartment, Model 1100 UV detector, and MSD bench top mass spectrometer (Hewlett-Packard, Palo Alto, CA, USA) with ESI interface. LC was performed on a 150 x 2.1 mm, I.D. column packed with 5 µm Symmetry C18 (Waters). For optimization of ion source parameters, a calibration standard (Hewlett-Packard) was introduced with an automated delivery system. The optimization of drying gas and nebulizer gas was done to introduce fexofenadine standard solution at 0.25 mL/min. The instrument was used in the positive ion mode using the following operating conditions: drying gas, 11 L/min at 350°C; nebulizer gas, 30 p.s.i.; capillary voltage, 2500 V; fragmentor voltage, 140 V; multiplier gain, 1 (1 p.s.i. = 6894.76 Pa). Full scan acquisitions were mode over a mass range of 150-650 u. Selective ion monitoring (SIM) was performed at m/z 502 ($[M+H]^+$ of fexofenadine), the dwell time was 0.58 s.

DMD Fast Forward. Published on February 2, 2006 as DOI: 10.1124/dmd.105.007559
This article has not been copyedited and formatted. The final version may differ from this version.

Results

Permeability of [^{14}C]Bepotastine and Fexofenadine in LLC-PK1 and LLC-GA5-COL150 Cells. The role of P-gp in bepotastine transport was assessed using the LLC-PK1 cells and LLC-GA5-COL150 cells that are stably transfected with human MDR1 gene. The results for the transcellular transport of [^{14}C]bepotastine, fexofenadine and [^{3}H]digoxin in LLC-PK1 and LLC-GA5-COL150 monolayers, along with the flux ratios, are summarized in Table 1. The flux ratios of [^{14}C]bepotastine (5 μM), fexofenadine (5 μM) and [^{3}H]digoxin (20 nM) in LLC-GA5-COL150 cells were significantly greater than those in LLC-PK1, showing that the basal-to-apical (B-to-A) flux exceeded to those in the other direction in LLC-GA5-COL150 cells. The corrected flux ratio of [^{14}C]bepotastine in the presence of an excess bepotastine (500 μM) was lower than that of tracer concentration of [^{14}C]bepotastine (5 μM). Furthermore, the corrected flux ratio of [^{14}C]bepotastine declined in the presence of P-gp inhibitors such as cyclosporin A (10 μM) and verapamil (100 μM). These results indicated that bepotastine as well as fexofenadine is a substrate of human P-gp. However, in LLC-PK1 cells, the Papp of the apical-to-basal (A-to-B) and the basal-to-apical (B-to-A) of bepotastine were approximately 8-, and 6-times higher than those of the apical-to-basal (A-to-B) and basal-to-apical (B-to-A) transport of fexofenadine, respectively. The apparent difference in transport in the absence of P-gp between bepotastine and fexofenadine may be ascribed to the difference in the intrinsic membrane permeability.

Stimulation of ATP Hydrolysis by Bepotastine and Verapamil. The affinity of bepotastine (A) and verapamil (B) to P-gp was estimated by ATPase activity assay. Figure 2 shows the concentration-dependent stimulation of vanadate-sensitive P-gp ATPase activity. The Km, Vmax and Vmax/Km values of P-gp-mediated ATP hydrolysis by bepotastine were 1.25 ± 0.02 mM, 108 ± 2.2 nmol/min/mg protein and 0.087 ± 0.003 mL/min/mg protein, respectively. These data suggested that bepotastine has low affinity to P-gp. In contrast, verapamil strongly stimulated the ATP hydrolysis activity. The Km, Vmax and Vmax/Km values of P-gp-mediated ATP hydrolysis by verapamil were 6.10 ± 0.23 μM, 93.4 ± 2.7 nmol/min/mg protein and 15.3 ± 0.1 mL/min/mg protein, respectively. The

estimated Km value of verapamil to P-gp showed a good agreement with the previous report (4.06 μM) (Adachi et al., 2001).

Brain Penetration of [^{14}C]Bepotastine in P-gp KO, and WT Mice. In order to evaluate the involvement of P-gp in the *in vivo* brain penetration of bepotastine, the radioactivity of [^{14}C]bepotastine was measured after intravenous bolus administration of [^{14}C]bepotastine at a dose of 0.8 mg/kg to wild-type (WT) and *mdr1a/1b(-/-)* (P-gp KO) mice. The whole-body autoradiograms at 60 min after dosing are shown in Figure 3A. The distribution of radioactivity was visually similar between WT and P-gp KO mice, excluding the central nervous system tissues. The radioactivity in central nervous system tissues of P-gp KO mice was high as compared with that of WT mice. The plasma total concentration of [^{14}C]bepotastine in WT and P-gp KO mice at 6 min after dosing were 580 ± 54.6 ng/mL and 467 ± 50.1 ng/mL, respectively, and those in WT and P-gp KO mice at 60 min after dosing were 260 ± 15.8 ng/mL and 280 ± 9.4 ng/mL, respectively. The plasma protein binding of WT and P-gp KO mice were 41.1 ± 0.8% and 45.9 ± 1.2%, respectively. The estimated plasma free concentration of [^{14}C]bepotastine in WT at 6 and 60 min after dosing were 341 ± 32.1 ng/mL and 153 ± 9.3 ng/mL, respectively and those in P-gp KO mice were 253 ± 27.1 ng/mL and 152 ± 5.1 ng/mL, respectively. The brain-to-plasma free concentration ratio (Kp,f) in cerebrum in WT mice at 6 and 60 min after dosing were 0.049 ± 0.003 and 0.097 ± 0.004, respectively, and those in cerebellum were 0.065 ± 0.007 and 0.119 ± 0.004, respectively. In contrast, those in P-gp KO mice at 6 and 60 min after dosing were 0.108 ± 0.001 and 0.305 ± 0.015, respectively, and those in cerebellum were 0.130 ± 0.006 and 0.353 ± 0.019, respectively. The values of Kp,f in P-gp KO mice were 2.2- and 3.1-times higher than those in WT mice at 6 and 60 min after iv injection, respectively (Fig. 3B). Therefore, limited brain penetration of bepotastine could be directly due to the P-gp-mediated efflux transport out of central nervous system tissues.

Site-specific Absorption of [^{14}C]Bepotastine in Rat Gastrointestinal Tract. The intestinal absorption

of bepotastine was evaluated in terms of disappearance of [^{14}C]bepotastine from *in situ* closed loops of stomach, small intestine, and colon in 30 min. The absorption of [^{14}C]bepotastine in stomach and colon were relatively small, and it seems to be absorbed predominantly from the small intestine (Fig. 4A). The absorption from proximal region of small intestine (83.4 ± 3.1% of dose) was higher than those from middle and distal regions. These results indicated that bepotastine exhibited regional difference in the intestinal absorption from gastrointestinal tract and the proximal region is a major site for intestinal absorption of bepotastine. The effects of verapamil (10 mM) on [^{14}C]bepotastine absorption at proximal and distal region in small intestine are shown in Figure 4B and Table 2, 3. The absorption of [^{14}C]bepotastine from proximal region in the presence and absence of verapamil were 63.0 ± 2.4% and 72.4 ± 1.1%, respectively and those from distal region were 10.9 ± 1.2% and 62.7 ± 2.8%, respectively. Interestingly, the regional difference of [^{14}C]bepotastine absorption at small intestine disappeared in the presence of P-gp inhibitor verapamil.

Comparison of Intestinal Absorption at Proximal and Distal Region between Bepotastine and Fexofenadine. Figure 5 compares the intestinal absorption of [^{14}C]bepotastine, fexofenadine and [^{14}C]mannitol (paracellular marker) from proximal and distal regions of small intestine by *in situ* loop method for 30 min. The absorption rates of [^{14}C]bepotastine from proximal and distal regions were 65.6 ± 3.3% and 10.0 ± 2.2%, respectively. On the contrary, the absorption rates of fexofenadine from proximal and distal regions were 8.5 ± 0.3% and 4.2 ± 1.2%, respectively, and were similar to those of [^{14}C]mannitol. The fractional absorptions of [^{14}C]bepotastine in the proximal and distal regions were 7.7-, and 2.4-times larger than those of fexofenadine.

Effect of P-gp Inhibitors on Intestinal Absorption of [^{14}C]Bepotastine and Fexofenadine at Proximal and Distal Small Intestinal Regions. The impact of P-gp-mediated efflux transport on intestinal absorption of bepotastine was examined by comparing the effects of P-gp inhibitors on fexofenadine. The *ka* value of [^{14}C]bepotastine (1 μM) at proximal region was approximately 8-times

larger than that at distal region. The absorption of [^{14}C]bepotastine was not affected by the first-generation H1-antagonist diphenhydramine (20 mM), which induces the sedation, while the same concentration of bepotastine significantly increased the absorption rate constant of [^{14}C]bepotastine from 1.98 to 2.84 hr^{-1}. In contrast, the *ka* value of [^{14}C]bepotastine increased 1.7- and 1.3-times at proximal region in the presence of P-gp inhibitors such as cyclosporin A and verapamil, respectively. At the distal region, the *ka* values of [^{14}C]bepotastine were increased 7.4-, 7.8- and 4.9-times in the presence of P-gp inhibitors, cyclosporin A, verapamil and quinidine, respectively. In the case of fexofenadine, the *ka* values at proximal and distal regions were increased approximately 4-times in the presence of P-gp inhibitors with a comparative effect in proximal and distal regions, while the effects of P-gp inhibitors were more significant in distal region in the case of bepotastine.

Discussion

The sedation of H1-antagonist is well known as an adverse reaction in central nervous system and the seriousness of the sedation is due to the brain penetration, the affinity and/or selectivity to H1-receptor and receptor occupation (Yanai et al., 1999; Tagawa et al., 2001). Among the factors that determine the brain concentration are physicochemical properties of drugs and the transporters at the BBB. The first-generation H1-antagonist mepyramine is taken up via carrier-mediated transport system, resulting in a severe central nervous system side effect (Yamazaki et al.,1994a and 1994b). However, second-generation H1-antagonists such as fexofenadine, ebastine, epinastine and cetirizine exhibit limited distribution into brain due to a P-gp-mediated efflux transport (Tamai et al., 2000; Polli et al., 2003; Ishiguro et al., 2004; Tahara et al., 2005). The influence of P-gp-mediated efflux transport on intestinal absorption process of therapeutic agents is also important, because P-gp is highly expressed in the small intestine, while the impact of P-gp-mediated efflux transport is variable among agents (Varma at al., 2005). Bepotastine is a non-sedative H1-antagonist and it shows the limited distribution into brain, while it is well absorbed after oral administration. Since the limited distribution of H1-antagonists is mainly explained by the involvement of P-gp, bepotastine may also be a substrate of P-gp. So, bepotastine could be a useful compound to clarify the apparent difference of the effect of P-gp between brain and small intestine. In the present study, we investigated the mechanism of the limited distribution into brain with a high intestinal absorption of bepotastine.

First of all, an involvement of P-gp-mediated efflux transport of bepotastine was assessed by *in vitro* transport studies by human P-gp overexpressing LLC-GA5-COL150 cells and *in vivo* pharmacokinetic studies by P-gp KO mice. The basal-to-apical transport of [^{14}C]bepotastine (5 μM), fexofenadine (5 μM) and [^{3}H]digoxin (20 nM) showed 4.0-, 3.9-, and 19.5-times higher permeability than that of apical-to-basal transport in the LLC-GA5-COL150 cells, whereas the directional transports of these compounds were not observed in the LLC-PK1 cells (Table 1). The corrected flux ratio (CFR) of [^{14}C]bepotastine, fexofenadine and [^{3}H]digoxin were 5.26, 3.91 and 11.36, respectively. The value of CFR of bepotastine was higher than unity as the same as those of fexofenadine and digoxin.

Furthermore, the directional transport of [^{14}C]bepotastine in the LLC-GA5-COL150 cells disappeared in the presence of P-gp inhibitors such as cyclosporin A and verapamil. The whole body autoradiograms showed that the radioactivity level of [^{14}C]bepotastine in the brain of WT mice was lower than that in P-gp KO mice. From pharmacokinetic analysis, the brain-to-plasma free concentration ratio (Kp,f) in P-gp KO mice was 2.2- and 3.1-times higher than that in WT mice at 6 and 60 min after dosing, respectively. The plasma free concentration of [^{14}C]bepotastine in WT mice was lower than the Km value of bepotastine to P-gp. Accordingly, the P-gp function was not saturated in the endothelial cells of brain capillaries by bepotastine in plasma. Polli et al. (2003) previously reported the similar results for cetirizine and showed that the values of Kp,f of cetirizine in P-gp KO mice were 2.3- and 4.6-times higher compared to those in WT mice at 5 and 60 min after dosing, respectively. These results clearly demonstrated that bepotastine is a substrate of P-gp. It was previously reported that bepotastine has a high selectivity for the histamine H1-receptor in the central nervous system and the brain-to-plasma concentration ratio of bepotastine in rats and mice is lower than those of the other H1-antagonists (Kato et al., 1997; Tamai et al., 2000; Polli et al., 2003, Ishiguro et al., 2004). These observations suggested that bepotastine has a low permeability and/or binding properties to central nervous system tissues and these characteristics are explained by the involvement of P-gp, resulting in a low sedative effect.

Although the low brain distribution of bepotastine is explained by P-gp, it is apparently controversial with high bioavailability after oral administration, because the intestinal P-gp limits the intestinal membrane permeability. Accordingly, the characteristics of intestinal absorption of bepotastine were examined. The absorption of [^{14}C]bepotastine in rat gastrointestinal tract showed clear regional difference, with high absorption in the proximal part of small intestine (Fig.4A). The similar phenomenon has been reported in the absorption of P-gp substrates cyclosporin A and cilostazol (Tamura et al., 2003; Toyobuku et al., 2003). The regional difference of [^{14}C]bepotastine absorption was disappeared in the presence of P-gp inhibitors and an excess bepotastine (Fig.4B, Tables 2 and 3). Furthermore, the alteration of intestinal absorption of [^{14}C]bepotastine in the presence of P-gp inhibitors was more significant at the distal region than proximal region, whereas that of fexofenadine in the

presence of P-gp inhibitors at the distal region was comparable with that at proximal region (Fig.4B, Table 2 and 3). Since the apparent difference between bepotastine and fexofenadine is in the influx membrane permeability at proximal region of small intestine (Fig. 5), the influx membrane permeability would affect the oral bioavailability and cause the apparent difference of the effects of P-gp inhibitors.

Recently, the heterogeneous expression of P-gp mRNA and protein in intestine of rats and humans was reported with a higher expression of P-gp at the lower site compared with an upper site of small intestine (Mouly et al., 2003; Takara et al., 2003; Valenzuela et al., 2003; Zimmermann et al., 2005). This regional difference of expression levels of P-gp may contribute to the variation of impact of P-gp on the intestinal absorption among P-gp substrates. Fricker et al. (1996) previously reported that the decrease of the intestinal absorption of cyclosporine A markedly correlated to the expression of mRNA for P-gp over the gastrointestinal tract. The site-specific P-gp-mediated efflux transport for tacrolimus in rat small intestine was investigated, and the activity of P-gp-mediated efflux transport for tacrolimus showed good agreement with the site-specific expression of P-gp (Tamura et al., 2002, 2003). The drug concentration at the proximal region is highest as compared to the distal part after oral administration and P-gp-mediated efflux transport could have more chance to be saturated at the proximal region. In the case of bepotastine, the saturation of P-gp may not explain the high absorption at proximal site of small intestine because the initial concentration in the intestinal proximal site at therapeutic dose (10mg, b.i.d.) with 200 mL water is approximately 90 μM and bepotastine has a low affinity to P-gp with Km value of 1.25 mM. Accordingly, the regional difference in the intestinal absorption of bepotastine can be explained by a gradual increase of P-gp expression level from proximal to distal region. In other words, the variation of intrinsic influx permeability and the gradual increase of P-gp-mediated efflux activity in the small intestine may explain the variable effect of P-gp on oral bioavailability of P-gp substrates. From these observations, following points on the effects of P-gp could be elucidated; Firstly, P-gp substrates with high solubility and high membrane permeability are well absorbed due to the limited efflux transport by low abundance of P-gp expression at the proximal small intestine. Secondary, P-gp substrates with good membrane permeability yet poor solubility are affected by P-gp because they are not

absorbed well at the proximal site of small intestine. Thirdly, formulating the P-gp substrates as a slow-sustained release preparation may not improve the overall absorption because of extensive efflux along middle to distal region in small intestine due to the low drug concentration and the higher expression of P-gp.

The involvement of the influx transporter for intestinal absorption of H1-antagonist has been suggested. The uptake of diphenhydramine in Caco-2 cells was mediated by pH-dependent transport system (Mizuuchi et al., 1999). Furthermore, fexofenadine was transported not only by P-gp but also by an organic anion transporting polypeptide (oatp) family (Cvetkovic et al., 1999; Nozawa et al., 2004). Involvement of oatp transporters in fexofenadine absorption was also suggested by the reduction of intestinal absorption by the fruit juices in humans and rats (Dresser et al., 2002, 2005; Kamath et al., 2005). However, it is unclear why bepotastine has high membrane permeability at the proximal region in the small intestine as compared to fexofenadine because there is no experimental evidence of involvement of the influx transporter to intestinal absorption of bepotastine until now. Further study is needed to clarify the underlying molecular mechanism of influx transport of bepotastine in small intestine.

In conclusion, the anti-allergic agent bepotastine is a substrate of P-gp as much as fexofenadine and P-gp clearly limits the brain distribution of bepotastine, while P-gp effect on the bioavailability of bepotastine after oral administration is negligible by showing almost complete absorption. The lack of the effect of P-gp on bepotastine absorption may be explained by its high membrane permeability at the proximal region of small intestine, where the P-gp expression is minimal at the proximal region of small intestine, while the effect of P-gp is extensive at the distal region of small intestine, where most of bepotastine has been already absorbed at the proximal region of small intestine. Such effect of P-gp on the bioavailablity of bepotastine is distinct from the low membrane permeable P-gp substrate fexofenadine. At present, the mechanism of the high permeability of bepotastine has not been clarified well, the influx permeability at the upper small intestine of orally administered drugs is an important factor to determine the apparent effect of P-gp on bioavailability.

Acknowledgments

We thank to Dr. Yusuke Tanigawara at Keio University Hospital and Dr. Kazumitsu Ueda at Kyoto University for kindly providing LLC-GA5-COL150 cells, and thank to Masaaki Takemura at GenoMembrane, Inc., for fruitful advice, and thanks to Masao Yamanouchi and Masakatsu Takahashi for their helpful animal experiment and excellent technical assistance of construction of whole-body autoradiograms.

References

Adachi Y, Suzuki H, and Sugiyama Y (2001) Comparative studies on *in vitro* methods for evaluating *in vivo* function of MDR1 P-glycoprotein. *Pharm Res* 18: 1660-1668.

Artursson P (1990) Epithelial transport of drugs in cell culture. I: A model for studying the passive diffusion of drugs over intestinal absorptive (Caco-2) cells. *J Pharm Sci* **79:** 476-482.

Cvetkovic M, Leake B, Fromm MF, Wilkinson GR, and Kim RB (1999) OATP and P-glycoprotein transporters mediate the cellular uptake and excretion of fexofenadine. *Drug Metab Dispos* **27:** 866-871.

Dresser GK, Bailey DG, Leake BF, Schwarz UI, Dawson PA, Freeman DI, and Kim RB (2002) Fruit juices inhibit organic anion transporting polypeptide-mediated drug uptake to decrease the oral availability of fexofenadine. *Clin Pharmacol Ther* **71:** 11-20.

Dresser GK, Kim RB, and Bailey DG (2005) Effect of grapefruit juice volume on the reduction of fexofenadine bioavailability: possible role of organic anion transporting polypeptides. *Clin Pharmacol Ther* **77:** 170-177.

Fricker G, Drewe J, Huwyler J, Gutmann H, and Beglinger C (1996) Relevance of p-glycoprotein for the enteral absorption of cyclosporin A: in vitro-in vivo correlation. *Br J Pharmacol* **118:** 1841-1847

Fujii T, Matsumoto S, Amejima H, Hatoyama T, Nakao M, Kagemoto A, Tanaka K, and Miyazaki H (1994) Absorption, distribution, metabolism and excretion of [^{14}C]ebastine after a single administration in rats. *Arzneimittelforschung* **44:** 527-538.

Honda H, Murata K, Hamazaki A, Sakamoto O, Ueno H, and Fujiwara H (1997) Inhibitory effect of betotastine on anaphylactic and histamine-induced reactions in guinea pig. *Jpn Pharmacol Ther* **25:** 879-888.

Ishiguro N, Nozawa T, Tsujihata A, Saito A, Kishimoto W, Yokoyama K, Yotsumoto T, Sakai K, Igarashi T, and Tamai I (2004) Influx and efflux transport of H1-antagonist epinastine across the blood-brain barrier. *Drug Metab Dispos* **32:** 519-24.

Kadosaka T, Shiraishi K, Mizuuchi H, Maki T, Banno K, and Sato T (1997) Phase I study of TAU-284:

Repeated oral administration in healthy male volunteers. *J Clin Therap Med* **13:** 1155-1168.

Kamath AV, Yao M, Zhang Y, and Chong S (2005) Effect of fruit juices on the oral bioavailability of fexofenadine in rats. *J Pharm Sci* **94:** 233-239.

Kato M, Nishida A, Aga Y, Kita J, Kudo Y, Narita H, and Endo T (1997) Pharmacokinetic and pharmacodynamic evaluation of central effect of the novel antiallergic agent betotastine besilate. *Arzneimittelforschung* **47:** 1116-1124.

Lin JH, and Yamazaki M (2003) Clinical relevance of P-glycoprotein in drug therapy. *Drug Metab Rev* **35:** 417-454.

Mizuuchi H, Katsura T, Saito H, Hashimoto Y, and Inui KI (1999) Transport characteristics of diphenhydramine in human intestinal epithelial Caco-2 cells: Contribution of pH-dependent transport system. *J Pharmacol Exp Ther* **290:** 388-392.

Mouly S, and Paine MF (2003) P-glycoprotein increases from proximal to distal regions of human small intestine. *Pharm Res* **20:** 1595-1599.

Nicholson AN (1983) Antihistamines and sedation. *Lancet* **2:** 211-212.

Nozawa T, Imai K, Nezu J, Tsuji A, and Tamai I (2004) Functional characterization of pH-sensitive organic anion transporting polypeptide OATP-B in human. *J Pharmacol Exp Ther* **308:** 438-445.

Ohashi R, Tsukimoto M, Nakamura S, Ohtsuka M, Hayashi K, Nishiyama S, Hanawa S, Mitsugi K, and Esumi Y (1997) Pharmacokinetic study of betotastine besilate (TAU-284) (I): absorption, distribution, metabolism and excretion after a single oral administration. *Xenobio Metabol and Dispos* **12:** 417-438.

Polli JW, Baughman TM, Humphreys JE, Jordan KH, Mote AL, Salisbury JA, Tippin TK, and Serabjit-Singh CJ (2003) P-glycoprotein influences the brain concentrations of cetirizine (Zyrtec), a second-generation non-sedating antihistamine. *J Pharm Sci* **92:** 2082-2089.

Sakai A, Kikuchi M, Yato N, Kikkawa S, Saito N, and Narita H (1997) Inhibitory effect of betotastine besilate on antigen-induced airway eosinophil infiltration and peripheral blood eosinophilia in mice. *Arzneimittelforschung* **47:** 954-958.

Schinkel A H, Smit J J M, van Tellingen O, Beijnen J H, Wagenaar E, van Deemter L, Mol C A A M, van der Valk M A, Robanus-Mandaag E C, te Riele H P J, Berns A J, and Borst P (1994): Disruption of the mouse mdr1a P-glycoprotein gene leads to a deficiency in the blood-brain barrier and to increased sensitivity to drugs. *Cell* **77:** 491-502.

Tagawa M, Kano M, Okamura N, Higuchi M, Matsuda M, Mizuki Y, Arai H, Iwata R, Fujii T, Komemushi S, Ido T, Itoh M, Sasaki H, Watanabe T, and Yanai K (2001) Neuroimaging of histamine H1-receptor occupancy in human brain by positron emission tomography (PET): a comparative study of ebastine, a second-generation antihistamine, and (+)-chlorpheniramine, a classical antihistamine. *Br J Clin Pharmacol* **52:** 501-509.

Tahara H, Kusuhara H, Fuse E, and Sugiyama Y (2005) P-glycoprotein plays a major role in the efflux of fexofenadine in the small intestine and blood-brain barrier, but only a limited role in its biliary excretion. *Drug Metab Dispos* **33:** 963-968.

Takara K, Ohnishi N, Horibe S, and Yokoyama T (2003) Expression profiles of drug-metabolizing enzyme CYP3A and drug efflux transporter multidrug resistance 1 subfamily mRNAs in small intestine. *Drug Metab Dispos* **31:** 1235-1239.

Tamai I, Kido Y, Yamashita J, Sai Y, and Tsuji A (2000) Blood-brain barrier transport of H1-antagonist ebastine and its metabolite carebastine. *J Drug Target* **8:** 383-393.

Tamura S, Ohike A, Ibuki R, Amidon GL, and Yamashita S (2002) Tacrolimus is a class II low-solubility high-permeability drug: the effect of P-glycoprotein efflux on regional permeability of tacrolimus in rats. *J Pharm Sci* **91:** 719-729.

Tamura S, Tokunaga Y, Ibuki R, Amidon GL, Sezaki H, and Yamashita S (2003) The site-specific transport and metabolism of tacrolimus in rat small intestine. *J Pharmacol Exp Ther* **306:** 310-316.

Tanigawara Y, Okamura N, Hirai M, Yasuhara M, Ueda K, Kioka N, Komano T, and Hori R (1992) Transport of digoxin by human P-glycoprotein expressed in a porcine kidney epithelial cell line (LLC-PK1). *J Pharmacol Exp Ther* **263:** 840-845

Toyobuku H, Tamai I, Ueno K, and Tsuji A (2003) Limited influence of P-glycoprotein on small-intestinal

absorption of cilostazol, a high absorptive permeability drug. *J Pharm Sci* **92:** 2249-2259.

Tsuji A, Terasaki T, Takabatake Y, Tenda Y, Tamai I, Yamashima T, Moritani S, Tsuruo T, and Yamashita J (1992) P-glycoprotein as the drug efflux pump in primary cultured bovine brain capillary endothelial cells. *Life Sci* **51:** 1427-1437.

Ueda K, Okamura N, Hirai M, Tanigawara Y, Saeki T, Kioka N, Komano T, and Hori R (1992) Human P-glycoprotein transports cortisol, aldosterone, and dexamethasone, but not progesterone. *J Biol Chem* **267:** 24248-24252.

Valenzuela B, Nacher A, Ruiz-Carretero P, Martin-Villodre A, Lopez-Carballo G, and Barettino D (2004) Profile of P-glycoprotein distribution in the rat and its possible influence on the salbutamol intestinal absorption process. *J Pharm Sci* **93:** 1641-1648.

Varma MV, Sateesh K, and Panchagnula R (2005) Functional role of P-glycoprotein in limiting intestinal absorption of drugs: contribution of passive permeability to P-glycoprotein mediated efflux transport. *Mol Pharm* **2:** 12-21.

Yamazaki M, Terasaki T, Yoshioka K, Nagata O, Kato H, Ito Y, and Tsuji A (1994a) Carrier-mediated transport of H1-antagonist at the blood-brain barrier: mepyramine uptake into bovine brain capillary endothelial cells in primary monolayer cultures. *Pharm Res* **11:** 975-978.

Yamazaki M, Terasaki T, Yoshioka K, Nagata O, Kato H, Ito Y, and Tsuji A (1994b) Carrier-mediated transport of H1-antagonist at the blood-brain barrier: a common transport system of H1-antagonists and lipophilic basic drugs. *Pharm Res* **11:** 1516-1518.

Yanai K, Okamura N, Tagawa M, Itoh M, and Watanabe T (1999) New findings in pharmacological effects induced by antihistamines: from PET studies to knock-out mice. *Clin Exp Allergy* **29 (Supp. 3):** 29-36.

Yato N, Murata T, Saito N, Sakai A, Kikuchi M, Tsuzurahara K, and Narita H (1997) Anti-allergic activity of Betotastine Besilate (TAU-284), New anti-allergic drug. *Folia Pharmacol Jpn* **110:** 19-29.

Zimmermann C, Gutmann H, Hruz P, Gutzwiller JP, Beglinger C, and Drewe J (2005) Mapping of multidrug resistance gene 1 and multidrug resistance-associated protein isoform 1 to 5 mRNA

expression along the human intestinal tract. *Drug Metab Dispos* **33:** 219-24

Legends for Figures

FIG. 1. *Chemical structures of [^{14}C]bepotastine and fexofenadine. *: ^{14}C-labeled position*

FIG. 2. *Concentration-dependent stimulation of P-gp ATPase activity in isolated membrane from human P-gp expressing cells by bepotastine (A) and verapamil (B).*

The ATPase activity of isolated membranes was determined by measuring vanadate sensitive inorganic phosphate liberation, using 4 mM MgATP, as described Materials and Methods. Data are shown as the mean ± SEM of independent three experiments. The vanadate sensitive ATP hydrolysis was determined by subtracting the value obtained with the vanadate co-incubated membrane fraction from vanadate-free membrane fraction.

FIG. 3. *Brain penetration of [^{14}C]bepotastine in P-gp knockout (KO) and wild-type (WT) mice.*

The whole-body autoradiograms (A) and brain-to-plasma free concentration ratio (B) of [^{14}C]bepotastine were evaluated at 6 or 60 min after intravenous administration of [^{14}C]bepotastine to P-gp KO (open column) and WT (closed column) mice at a dose of 0.8 mg/45 μCi/kg. At 6 and 60 min after dosing, mice were sacrificed and tissues were isolated and weighed for analysis of Kp,f. The data are shown as the mean ± SEM of three animals. The statistical differences between P-gp KO and WT mice were assessed by Student's *t* test ($P < 0.05$).

FIG. 4. *Intestinal absorption of [^{14}C]bepotastine from various sites of gastrointestinal tract of rats.*

The absorption of [^{14}C]bepotastine (2 mM) at stomach, small intestine (proximal, mean and distal region) and colon (A) and the effect of verapamil (10 mM) on the [^{14}C]bepotastine (1 μM) absorption at proximal and distal site of small intestine (B) were evaluated by the residual radioactivity in the closed loops (8-cm long small intestine and colon) at 30 min after injection of test compound. Each value represents the mean ± SEM of three animals. * Significantly differences of the absorption rate of [^{14}C]bepotastine between at the intestinal proximal site and at the other site were calculated by Student's *t*

test ($P < 0.05$). ** Significantly differences of the absorption rate of [^{14}C]bepotastine between in the absence of verapaml and in the presence of verapamil were calculated by Student's *t* test ($P < 0.05$).

FIG. 5. *Comparison of intestinal absorption at proximal (A) and distal (B) regions between [^{14}C]bepotastine and fexofenadine in rats.*

The intestinal absorption of [^{14}C]bepotastine (1 μM), fexofenadine (370 μM) and [^{14}C]mannitol (2 μM) was evaluated by the residual amount in the intestinal closed loops in the proximal and distal regions (8-cm) at 30 min after injection of test compounds. Each value represents the mean ± SEM of three animals.

TABLE 1

Kinetic Parameters for the Transcellular Transport in LLC-PK1 and LLC-GA5-COL150 Cells

The transport of [^{14}C]bepotastine, fexofenadine and [^{3}H]digoxin across LLC-PK1 and LLC-GA5-COL150 monolayers in the presence or absence of P-gp inhibitor were evaluated the amount transported to the receiver side in the apical-to-basal (A-to-B) and basal-to-apical (B-to-A) direction for 2 hours after adding the drugs. Each value represents the mean ± SEM of three to six experiments.

Condition	LLC-PK1			LLC-GA5-COL150			
	Papp (1 x 10^{-6} cm/sec)			Papp (1 x 10^{-6} cm/sec)			
	A-to-B	B-to-A	Flux Ratio	A-to-B	B-to-A	Flux Ratio	CFR
[^{14}C]Bepotastine (5 μM)	5.87 ± 0.14	4.51 ± 0.31	0.77 ± 0.03	1.57 ± 0.04	6.30 ± 0.26	4.00 ± 0.10 *	5.26 ± 0.22
[^{14}C]Bepotastine (500 μM)	5.18 ± 0.13	3.98 ± 0.27	0.77 ± 0.03	1.81 ± 0.04	5.56 ± 0.23	3.06 ± 0.07 *	4.03 ± 0.19 **
[^{14}C]Bepotastine + Cyclosporin A (5 μM) (10 μM)	4.78 ± 0.35	3.93 ± 0.23	0.82 ± 0.01	2.81 ± 0.07	3.70 ± 0.66	1.31 ± 0.23	1.60 ± 0.32 **
[^{14}C]Bepotastine + Verapamil	4.65 ± 0.21	3.99 ± 0.18	0.86 ± 0.04	2.43 ± 0.14	3.53 ± 0.29	1.45 ± 0.25	1.71 ± 0.43 **

(5 μM)	(100 μM)						
Fexofenadine (5 μM)	0.77 ± 0.02	0.80 ± 0.04	1.04 ± 0.05	0.19 ± 0.03	0.72 ± 0.01	3.90 ± 0.63 *	3.91 ± 1.04
[^{3}H]Digoxin (20 nM)	3.66 ± 0.08	6.30 ± 0.35	1.74 ± 0.09	0.78 ± 0.02	15.26 ± 0.51	19.49 ± 0.58 *	11.36 ± 0.08

* Statistical difference of the flux ratio between LLC-PK1 and LLC-GA5-COL150 cells was assessed by Student's *t* test ($p < 0.05$).

** Statistical difference of the corrected flux ratio compared to that of [^{14}C]bepotastine (5 μM) in the presence of P-gp inhibitor was assessed by Student's *t* test ($p < 0.05$)

DMD Fast Forward. Published on February 2, 2006 as DOI: 10.1124/dmd.105.007559
This article has not been copyedited and formatted. The final version may differ from this version.

TABLE 2

Influence of several drug on intestinal absorption of [^{14}C]bepotastine and fexofenadine at proximal region in rats.

The absorption at proximal region [^{14}C]bepotastine and fexofenadine in the presence or absence of several drugs were evaluated by the closed loop method. The data correspond to the intestinal absorption at proximal region within 30 min after injection to intestinal loop (8-cm). Each value represents the mean ± SEM of three animals. The values in parentheses represent the ratio of the apparent absorption rate constant (*ka*) by [^{14}C]bepotastine (1 μM), fexofenadine (370 μM) and [^{14}C]mannitol (2 μM).

Condition	Absorption Rate (% of Dose)	*ka* (hr^{-1})	
[^{14}C]Bepotastine (1 μM)	63.0 ± 2.4	1.98 ± 0.12	(1.00)
[^{14}C]Bepotastine (20 mM)	74.2 ± 5.9 *	2.84 ± 0.53	(1.43)
[^{14}C]Bepotastine (1 μM) + Diphenhydramine (20 mM)	57.1 ± 3.7	1.71 ± 0.18	(0.86)
[^{14}C]Bepotastine (1 μM) + Cyclosporin A (50 μM)	81.5 ± 2.1 *	3.40 ± 0.22 *	(1.71)
[^{14}C]Bepotastine (1 μM) + Verapamil (10 mM)	72.4 ± 1.1 *	2.58 ± 0.08	(1.30)
Fexofenadine (370 μM)	8.5 ± 0.3	0.18 ± 0.01	(1.00)
Fexofenadine (370 μM) + Cyclosporin A (50 μM)	29.9 ± 7.3 *	0.73 ± 0.22 *	(4.12)
Fexofenadine (370 μM) + Verapamil (10 mM)	24.9 ± 4.9 *	0.58 ± 0.13 *	(3.26)
[^{14}C]Mannitol (1 μM)	4.4 ± 1.2	0.09 ± 0.02	

* Statistical difference of the absorption rate (% of Dose) and the apparent absorption rate constant, *ka*, in the presence of excessive bepotastine and several drugs including P-gp inhibitors was assessed by Student's *t* test ($p < 0.05$).

TABLE 3

Influence of P-gp inhibitor on intestinal absorption of [^{14}C]bepotastine and fexofenadine at distal region in rats.

The absorption at distal region [^{14}C]bepotastine and fexofenadine in the presence or absence of P-gp inhibitor were evaluated by the closed loop method. The data correspond to the intestinal absorption at distal region within 30 min after injection to intestinal loop (8-cm). Each value represents the mean ± SEM of three animals. The values in parentheses represent the ratio of the apparent absorption rate constant (*ka*) by [^{14}C]bepotastine (1 μM), fexofenadine (370 μM) and [^{14}C]mannitol (2 μM).

Condition	Absorption Rate (% of Dose)	*ka* (hr^{-1})	
[^{14}C]Bepotastine (1 μM)	10.9 ± 1.2	0.26 ± 0.03	(1.00)
[^{14}C]Bepotastine (20 mM)	38.3 ± 2.0 *	0.97 ± 0.07 *	(3.79)
[^{14}C]Bepotastine (1 μM) + Cyclosporin A (50 μM)	59.7 ± 1.4	1.89 ± 0.07 *	(7.41)
[^{14}C]Bepotastine (1 μM) + Verapamil (10 mM)	62.7 ± 2.8 *	1.98 ± 0.15 *	(7.77)
[^{14}C]Bepotastine (1 μM) + Quinidine (10 mM)	46.0 ± 2.5 *	1.24 ± 0.09 *	(4.85)
Fexofenadine (370 μM)	4.2 ± 1.2	0.09 ± 0.03	(1.00)
Fexofenadine (370 μM) + Cyclosporin A (50 μM)	17.9 ± 0.9 *	0.40 ± 0.02 *	(4.58)
Fexofenadine (370 μM) + Verapamil (10 mM)	13.0 ± 3.2	0.28 ± 0.08 *	(3.27)
[^{14}C]Mannitol (1 μM)	3.5 ± 1.1	0.07 ± 0.03	

* Statistical difference of the absorption rate (% of Dose) and the apparent absorption rate constant, *ka*, in

the presence of excessive bepotastine and P-gp inhibitors was assessed by Student's *t* test ($p < 0.05$).

Fig.1

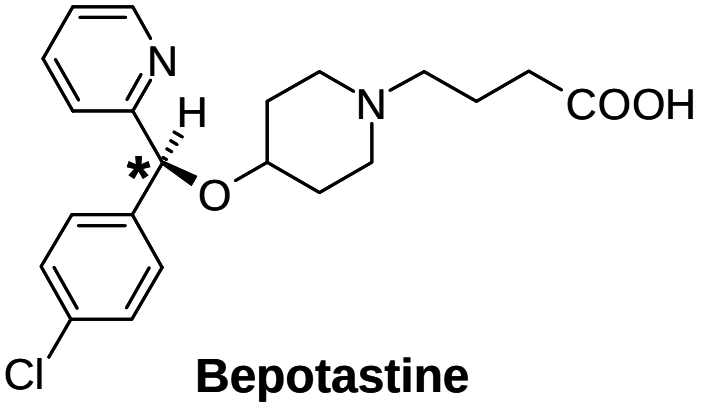

Bepotastine

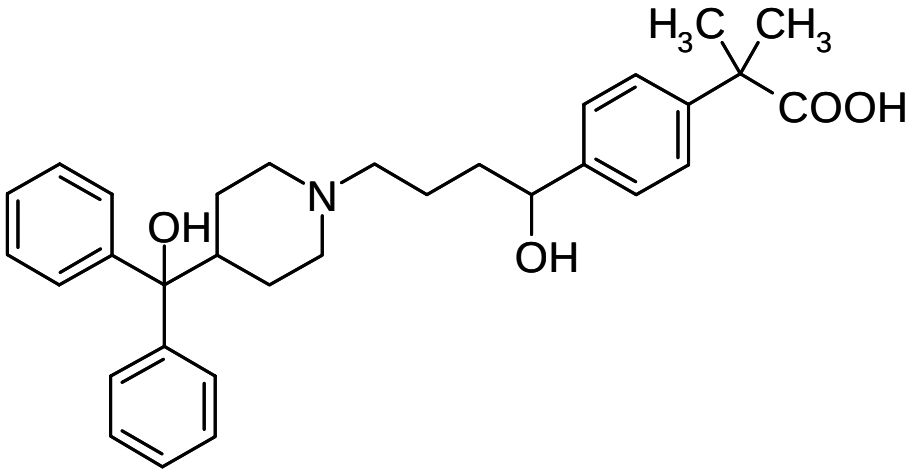

Fexofenadine

Fig.2

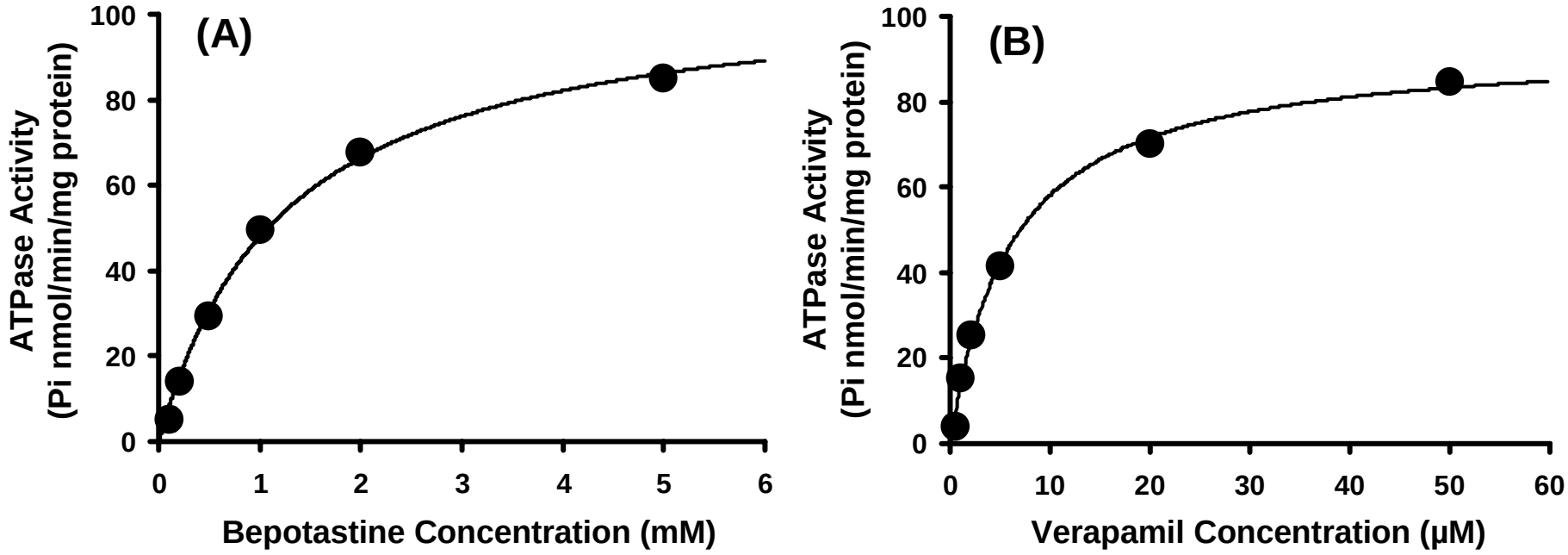

Fig.3

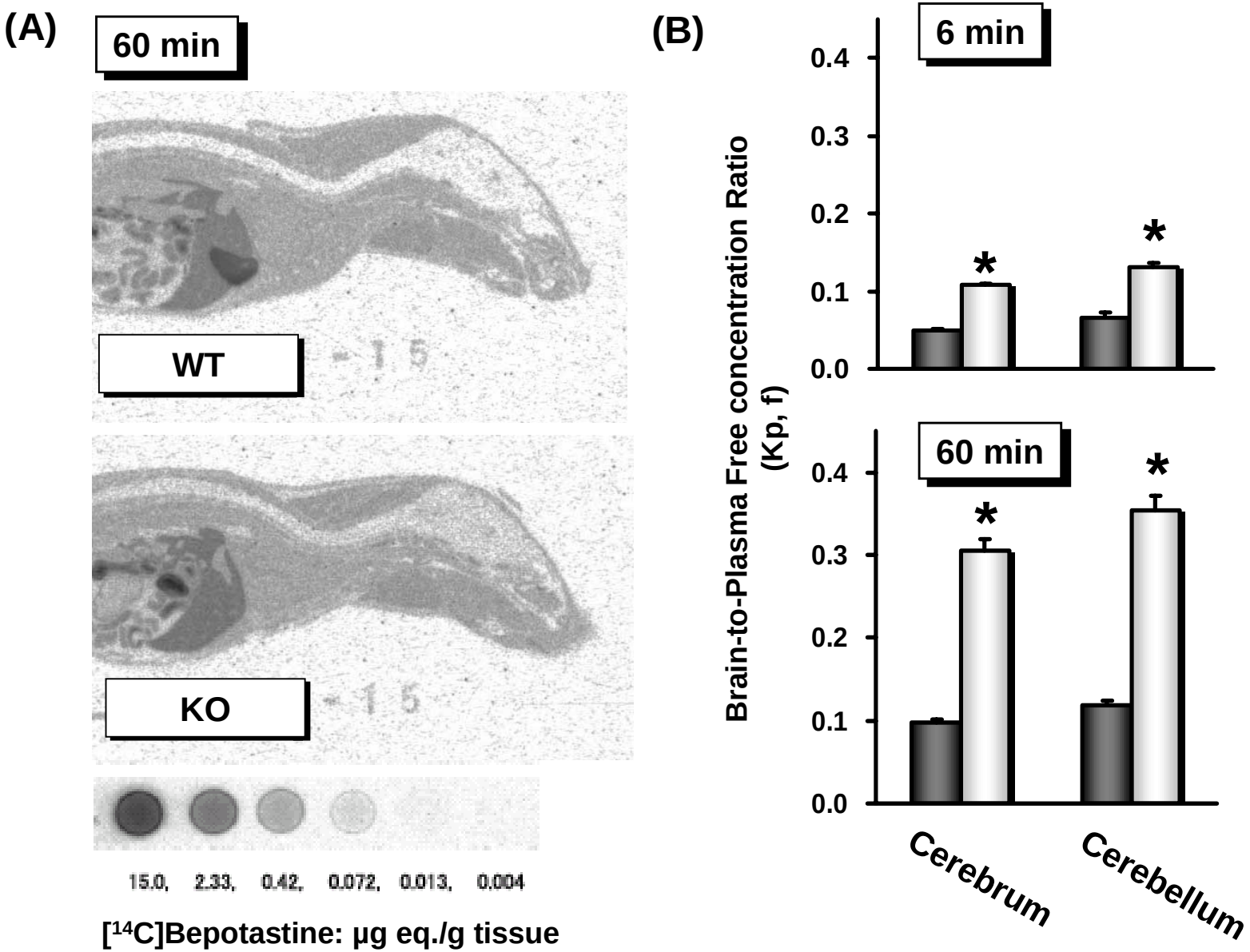

Fig.4

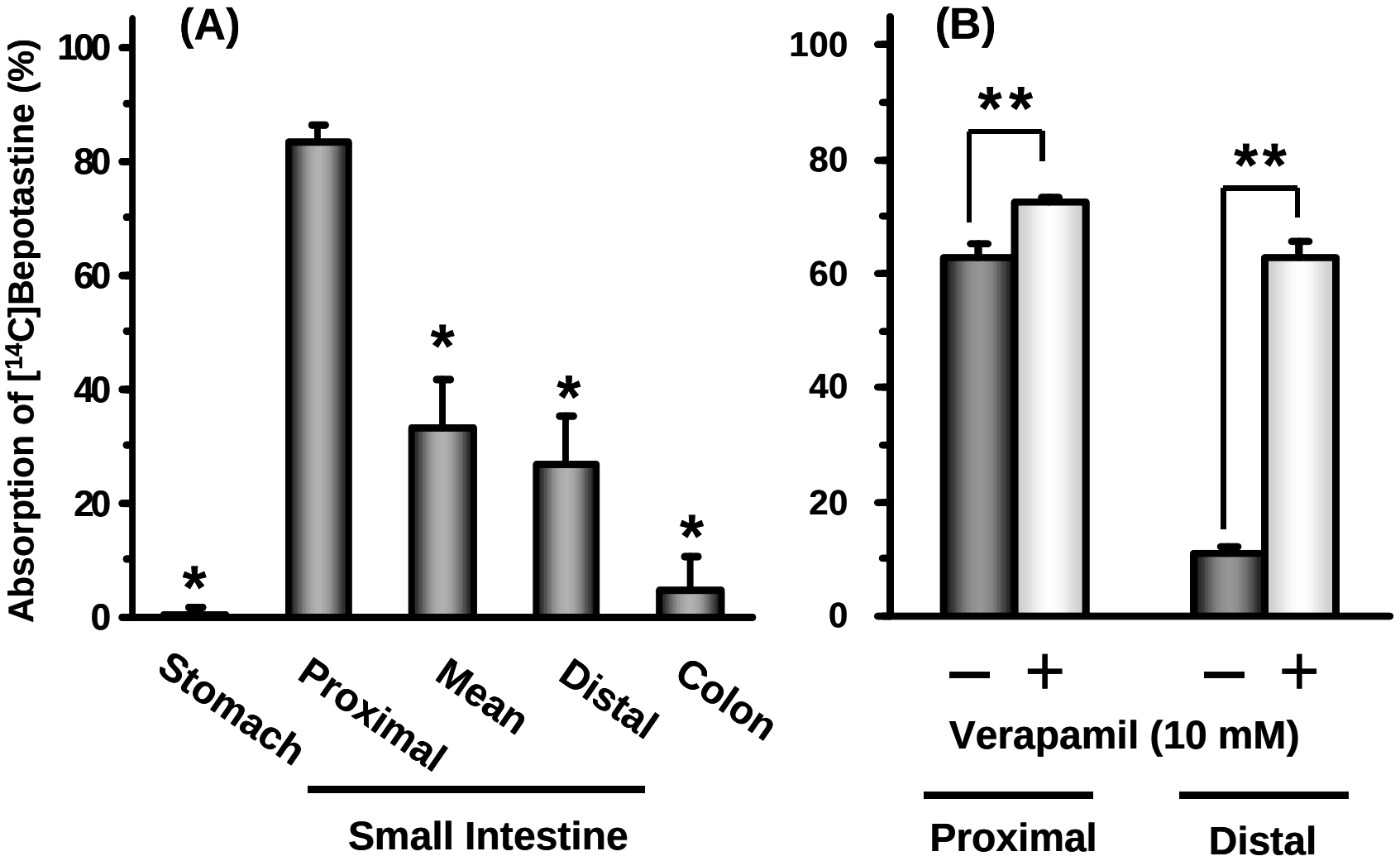

Fig.5